Fault Ride-Through of a DFIG Wind Turbine Using a Dynamic Voltage Restorer During Symmetrical and Asymmetrical Grid Faults

Christian Wessels, *Student Member, IEEE*, Fabian Gebhardt, *Student Member, IEEE*, and Friedrich Wilhelm Fuchs, *Senior Member, IEEE*

***Abstract*—The application of a dynamic voltage restorer (DVR) connected to a wind-turbine-driven doubly fed induction generator (DFIG) is investigated. The setup allows the wind turbine system an uninterruptible fault ride-through of voltage dips. The DVR can compensate the faulty line voltage, while the DFIG wind turbine can continue its nominal operation as demanded in actual grid codes. Simulation results for a 2 MW wind turbine and measurement results on a 22 kW laboratory setup are presented, especially for asymmetrical grid faults. They show the effectiveness of the DVR in comparison to the low-voltage ride-through of the DFIG using a crowbar that does not allow continuous reactive power production.**

***Index Terms*—Doubly fed induction generator (DFIG), dynamic voltage restorer (DVR), fault ride-through and wind energy.**

I. Introduction

THE INCREASED amount of power from decentralized renewable energy systems, as especially wind energy systems, requires ambitious grid code requirements to maintain a stable and safe operation of the energy network. The grid codes cover rules considering the fault ride-through behavior as well as the steady-state active power and reactive power production. The actual grid codes stipulate that wind farms should contribute to power system control like frequency and voltage control to behave similar to conventional power stations. A detailed review of grid code technical requirements regarding the connection of wind farms to the electrical power system is given in [1]. For operation during grid voltage faults, it becomes clear that grid codes prescribe that wind turbines must stay connected to the grid and should support the grid by generating reactive power to support and restore quickly the grid voltage after the fault.

Among the wind turbine concepts, turbines using the doubly fed induction generator (DFIG) as described in [2] and [3] are dominant due to its variable-speed operation, its separately controllable active and reactive power, and its partially rated power converter. But the reaction of DFIGs to grid voltage disturbances is sensitive, as described in [4] and [5] for symmetrical and unsymmetrical voltage dips, and requires additional protection for the rotor side power electronic converter.

Conventionally, a resistive network called crowbar is connected in case of rotor overcurrents or dc-link overvoltages to the rotor circuit, and the rotor side converter (RSC) is disabled as described in [6], [7] and [8]. But the machine draws a high short circuit current when the crowbar is activated, as described in [9], resulting in a large amount of reactive power drawn from the power network, which is not acceptable when considering actual grid code requirements. Thus, other protection methods have to be investigated to ride-through grid faults safely and fulfill the grid codes.

There are other proposed solutions using additional hardware for fault ride-through of a DFIG using additional hardware like a series dynamic resistance in the rotor in [10] or in the stator in [11] or using a series line side converter (LSC) topology as in [12].

Other approaches focus on limiting the rotor currents during transient grid voltage by changing the control of the RSC in order to avoid additional hardware in the system. The RSC can be protected by feedforward of the faulty stator voltage [13], by considering the stator flux linkage [14] or by using the measured stator currents as reference for the rotor current controllers [15]. Other publications focus on the improved performance during unsymmetrical grid voltage conditions [16]–[19]. A demagnetizing current is used to protect the converter in [20], but it becomes clear that during deep transient dips, a crowbar activation cannot be avoided, and thus, continuous reactive power control cannot be guaranteed.

If an external power electronic device is used to compensate the faulty grid voltage, any protection method in the DFIG system can be left out. Such a system is introduced in [21] and is called a dynamic voltage restorer (DVR) that is a voltage source converter connected in series to the grid to correct faulty line voltages. The advantages of such an external protection device are thus the reduced complexity in the DFIG system. The disadvantages are the cost and complexity of the DVR. Note that a DVR can be used to protect already installed wind turbines that do not provide sufficient fault ride-through behavior or to protect any distributed load in a microgrid.

Different DVR topologies are compared with respect to rating in power and voltage in [22]. A medium-voltage DVR is described in [23]. Control structures based on resonant controllers to compensate unsymmetrical voltages are presented

Manuscript received July 1, 2010; revised November 17, 2010 and November 23, 2010; accepted November 24, 2010. Date of current version May 13, 2011. Recommended for publication by Associate Editor Josep M. Guerrero.

The authors are with the Institute for Power Electronics and Electrical Drives, Christian-Albrechts-University of Kiel, Kaiserstr. 2, Kiel 24143, Germany (e-mail: chw@tf.uni-kiel.de; fwf@tf.uni-kiel.de).

Color versions of one or more of the figures in this paper are available online at http://ieeexplore.ieee.org.

Digital Object Identifier 10.1109/TPEL.2010.2099133

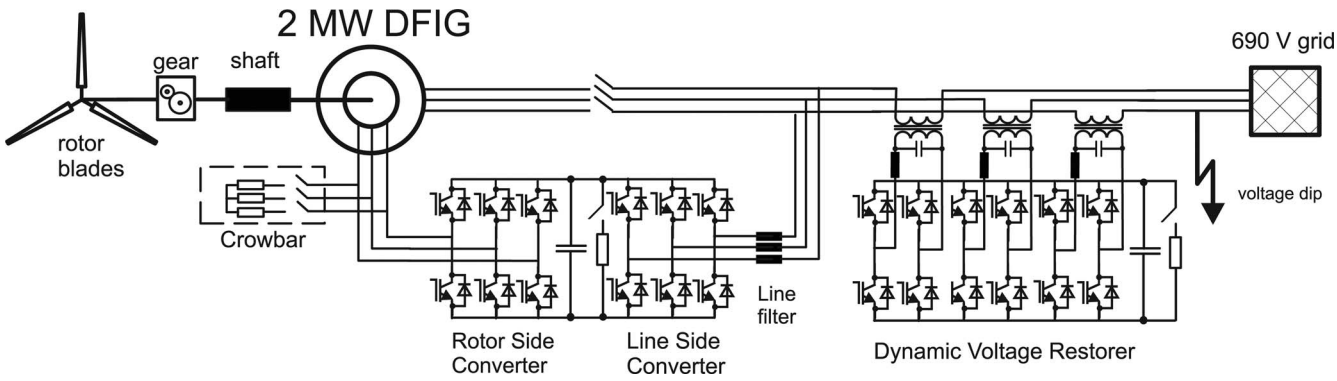

Fig. 1. Schematic diagram of DFIG wind turbine system with DVR.

in [24] and [25]. A DVR is used to provide fault ride-through capability for a squirrel cage induction generator in [26]. A DVR to protect a DFIG wind turbine has been presented in [27], but only symmetrical voltage dips have been investigated, and in [28], but the reactive power is not considered and measurement results do not cover transient grid faults.

In this paper, the application of a DVR that is connected to a wind-turbine-driven DFIG to allow uninterruptible fault ride-through of voltage dips fulfilling the grid code requirements is investigated. The DVR can compensate the faulty line voltage, while the DFIG wind turbine can continue its nominal operation as demanded in actual grid codes. Here, asymmetrical faults are investigated and measurement results under transient grid voltage dips on a 22 kW laboratory setup are presented. First results have been presented in [29], but a detailed analysis of DFIG behavior and DVR control is given here.

The structure is as follows. In Section II, the wind turbine system using a DFIG is described. An analysis of rotor voltage dynamics during transient symmetrical voltage dip and a description of the control structure and conventional crowbar protection are given. In Section III, the DVR electrical system and control using resonant controllers is described. Simulation results for a 2 MW wind turbine in Section IV and measurement results on a 22 kW laboratory test bench in Section V show the effectiveness of the proposed technique in comparison to the low-voltage ride-through of the DFIG using a crowbar. A conclusion closes the analysis.

II. DFIG

The investigated wind turbine system, as shown in Fig. 1, consists of the basic components like the turbine, a gear (in most systems), a DFIG, and a back-to-back voltage source converter with a dc link. A dc chopper to limit the dc voltage across the dc capacitor and a crowbar are included. The back-to-back converter consists of a RSC and a LSC, connected to the grid by a line filter to reduce the harmonics caused by the converter. A DVR is included to protect the wind turbine from voltage disturbances. Due to the short period of time of voltage disturbances, the dynamics of the mechanical part of the turbine will be neglected and the mechanical torque brought in by the wind is assumed to be constant.

A. Rotor Voltage Dynamics

A precise knowledge about amplitude and frequency of the rotor voltage is necessary to design and control the RSC. Therefore, equations for the rotor voltage in normal operation and under symmetrical stator voltage dip are derived in the following as in [4]. Afterwards, the rotor converter rating is taken into account.

From the per-phase equivalent circuit of the DFIG in a static-stator-oriented reference frame, the following stator and rotor voltage and flux equations can be derived:

$$\vec{v}_s = R_s\vec{i}_s + \frac{d\vec{\psi}_s}{dt} \tag{1}$$

$$\vec{v}_r = R_r\vec{i}_r + \frac{d\vec{\psi}_r}{dt} - j\Omega\vec{\psi}_r \tag{2}$$

$$\vec{\psi}_s = L_s\vec{i}_s + L_h\vec{i}_r \tag{3}$$

$$\vec{\psi}_r = L_r\vec{i}_r + L_h\vec{i}_s \tag{4}$$

where $\vec{\psi}$, $\vec{v}$, and $\vec{i}$ represent the flux, voltage, and current vectors, respectively. Subscripts s and r denote the stator and rotor quantities, respectively. $L_s = L_{s\sigma} + L_h$ and $L_r = L_{r\sigma} + L_h$ represent the stator and rotor inductance, L_h is the mutual inductance, R_s and R_r are the stator and rotor resistances, and Ω is the electrical rotor frequency.

By introducing the leakage factor $\sigma = 1 - (L_h^2/L_sL_r)$, the rotor flux can be described in dependence of the rotor current and the stator flux

$$\vec{\psi}_r = \frac{L_h}{L_s}\vec{\psi}_s + \sigma L_r\vec{i}_r. \tag{5}$$

By substituting (5) in (2), an equation for the rotor voltage can be obtained

$$\vec{v}_r = \frac{L_h}{L_s}\left(\frac{d}{dt} - j\Omega\right)\vec{\psi}_s + \left(R_r + \sigma L_r\left(\frac{d}{dt} - j\Omega\right)\right)\vec{i}_r \tag{6}$$

which consists of two parts. The first part is caused by the stator flux $\vec{\psi}_s$ that is given in normal operation by the constantly rotating vector

$$\vec{\psi}_s = \frac{V_s}{j\omega_s}e^{j\omega_s t}. \tag{7}$$

The second part of (6) is caused by the rotor current $\vec{i}_r$. The rotor resistance R_r and the leakage factor σ are often small, so the rotor voltage does not differ considerably from the part caused by the stator flux. Thus, the amplitude of the rotor voltage in normal condition V_{r0} can be calculated as

$$V_{r0} \approx V_s \frac{L_h}{L_s} \frac{\omega_r}{\omega_s} = V_s \frac{L_h}{L_s} s \tag{8}$$

where $s = 1 - (\Omega/\omega_s) = \omega_r/\omega_s$ describes the slip and ω_r the slip frequency.

The rotor voltage induced by the stator flux increases the most during a full symmetrical stator voltage dip. Under a symmetrical voltage dip, the stator voltage is reduced from normal amplitude V_1 to the faulty amplitude V_2 as described in (9)

$$\vec{v}_s = \begin{cases} V_1 e^{j\omega_s t}, & \text{for } t < t_0 \\ V_2 e^{j\omega_s t}, & \text{for } t \geq t_0 \end{cases} \tag{9}$$

$$\vec{\psi}_s = \begin{cases} \vec{\psi}_{s1} = \dfrac{V_1}{j\omega_s} e^{j\omega_s t}, & \text{for } t < t_0 \\ \vec{\psi}_{s2} = \dfrac{V_2}{j\omega_s} e^{j\omega_s t}, & \text{for } t \geq t_0. \end{cases} \tag{10}$$

Since the stator flux is a continuous value, it cannot follow the step function of the voltage. The evolution of the stator flux can be derived by solving the differential equation (11) (from (1) and (3), assuming $\vec{i}_r = 0$ due to its low influence on the rotor voltage)

$$\frac{d\vec{\psi}_s}{dt} = \vec{v}_s - \frac{R_s}{L_s} \vec{\psi}_s. \tag{11}$$

The solution consists of two parts. The first part is the steady-state stator flux after the voltage dip that is described by $\vec{\psi}_{s2}$ and the second part is the transition of the flux from $\vec{\psi}_{s1}$ to $\vec{\psi}_{s2}$ that is described by (12)

$$\vec{\psi}_s = \vec{\psi}_{s0} e^{-tR_s/L_s} = \vec{\psi}_{s0} e^{-t/\tau_s} \tag{12}$$

where $\vec{\psi}_{s0}$ is the difference of the stator flux before and after the voltage dip, described by $(V_1 - V_2)/j\omega_s$. Summarizing, the stator flux is given by the sum of the two parts

$$\vec{\psi}_s(t) = \frac{V_2}{j\omega_s} e^{j\omega_s t} + \frac{V_1 - V_2}{j\omega_s} e^{-t/\tau_s}. \tag{13}$$

When the dynamic stator flux from (13) is considered in the rotor voltage equation of (6) (neglecting $\vec{i}_r$ and $1/\tau_s$), the dynamic behavior of the rotor voltage under symmetrical voltage dip is described by (15)

$$\vec{v}_r = \frac{L_h}{L_s} \left(\frac{d}{dt} - j\Omega \right) \left(\frac{V_2}{j\omega_s} e^{j\omega_s t} + \frac{V_1 - V_2}{j\omega_s} e^{-t/\tau_s} \right) \tag{14}$$

$$= \frac{L_h}{L_s} \left(sV_2 e^{j\omega_s t} - (1-s)(V_1 - V_2) e^{-t/\tau_s} \right) \tag{15}$$

In a reference frame rotating at rotor frequency, the following rotor voltage is obtained:

$$\vec{v}_r = \frac{L_h}{L_s} \left(sV_2 e^{j\omega_r t} - (1-s)(V_1 - V_2) e^{-j\Omega t} e^{-t/\tau_s} \right). \tag{16}$$

The results of this analysis show that the rotor voltage during symmetrical voltage dip consists of two components. The first part is proportional to the slip and the remaining stator voltage; thus, for a deep voltage dip and a slip usually at -0.2, it is small. The frequency of the first part is the slip frequency (at a slip of -0.2, $\omega_r = 10\,\text{Hz}$). The second part of (16) has a high amplitude at $t = 0$ proportional to $(1 - s)$ and rotates at the electrical rotor frequency Ω (at a slip of -0.2, $\Omega = 60\,\text{Hz}$). The part is decaying exponentially with the stator time constant of τ_s. The maximum rotor voltage during symmetrical voltage dip will occur at the beginning of the fault ($t = 0$) and for a full dip ($V_2 = 0$)

$$V_{r,\max} \approx \frac{L_h}{L_s} (1 - s) V_1. \tag{17}$$

Note that (17) is an approximation of the maximum rotor voltage under the given circumstances. The RSC of a DFIG is rated for a part of the stator power, because the rotor power is approximately proportional to the slip $P_r \approx sP_s$ that is chosen usually between ± 0.3. The required amplitude of the rotor voltage is probably determined [with $L_h/L_s \approx 1$ in (8)] by

$$V_r = \frac{sV_s}{N_{sr}} \tag{18}$$

where N_{sr} is the stator to rotor turns ratio. The turns ratio is usually set at 1/2 or 1/3 in practical wind-turbine-driven DFIGs to make full use of the dc-link voltage and reduce the converters current rating. The required dc-link voltage can be determined by

$$m \frac{V_{dc}}{2} = V_r \tag{19}$$

where m is the modulation index of the pulse width modulation (PWM) technique. The value of the modulation index is 1.0 for the carrier-based sinusoidal PWM and 1.15 for the space vector modulation, both without overmodulation techniques [30].

The findings of the section enhance the understanding of rotor overcurrents during symmetrical grid voltage dip. Only if the RSC can provide a sufficient voltage level, controllability of rotor currents can be obtained. If the rotor voltage exceeds the converter voltage, high currents will flow through the diodes into the dc-link capacitor, damaging the insulated gate bipolar transistor (IGBT) or the dc capacitor.

B. Crowbar Protection

To protect the RSC from tripping due to overcurrents in the rotor circuit or overvoltage in the dc link during grid voltage dips, a crowbar is installed in conventional DFIG wind turbines, which is a resistive network that is connected to the rotor windings of the DFIG. The crowbar limits the voltages and provides a safe route for the currents by bypassing the rotor by a set of resistors. When the crowbar is activated, the RSCs pulses are disabled and the machine behaves like a squirrel cage induction machine directly coupled to the grid. The magnetization of the machine that was provided by the RSC in nominal condition is lost and the machine absorbs a large amount of reactive power from the stator, and thus, from the network [9], which can further reduce the voltage level and is not allowed in actual grid codes. Triggering of the crowbar circuit also means high stress

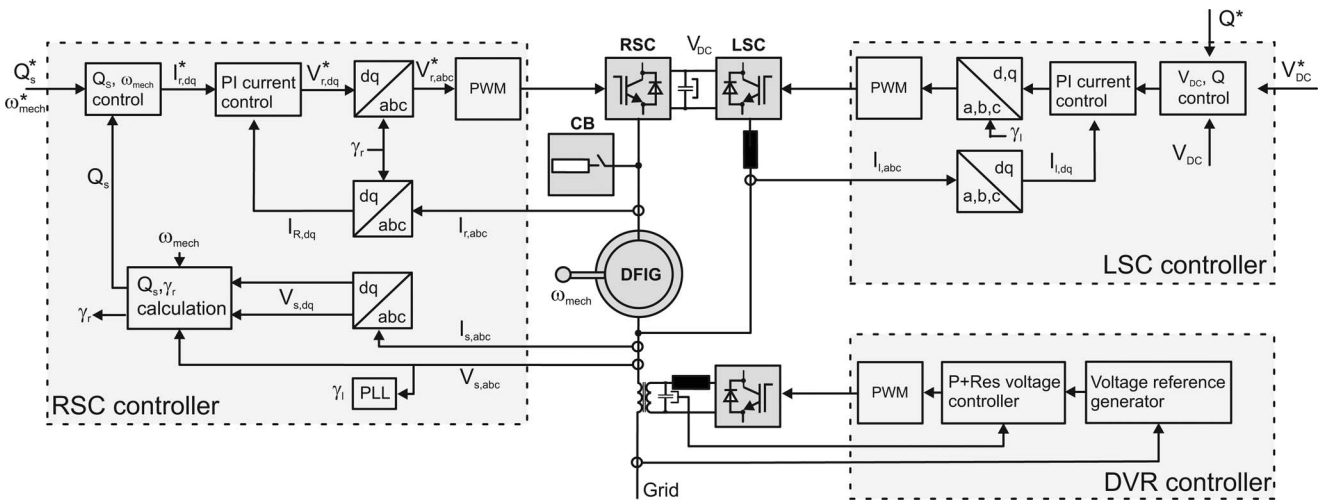

Fig. 2. Schematic diagram of DFIG wind turbine and DVR control structure.

to the mechanical components of the system as the shaft and the gear. Detailed analyses on the DFIG behavior during voltage dip and crowbar protection can be found in [6] and [9]. Thus, from network and machine mechanical point of view, a crowbar triggering should be avoided.

Anyway, to compare the presented technique here with a conventional DFIG wind turbine system protected by a crowbar circuit, simulation results including crowbar protection are examined. Therefore, the crowbar resistance is designed here. Crowbar resistances are also designed in [7] and [9].

There are two constraints that give an upper and a lower limit to the crowbar resistance. As a first constraint, the crowbar resistance should be high enough to limit the short-circuit rotor current $I_{r,\max}$. As the second constraint, the crowbar resistance should be low enough to avoid too high voltage in the rotor circuit. If the rotor phase voltage across the crowbar rises above the maximum converter voltage given in (18), high currents will flow through the antiparallel diodes of the converter. A crowbar resistance of $R_{\rm crow} = 150R_r$ is used in the simulations.

There are approaches limiting the operation time of the crowbar to return to normal DFIG operation with active and reactive power control as soon as possible like in [15] by injecting a demagnetizing current or in [8] using a threshold control.

In the laboratory setup, a passive crowbar circuit is used that is triggered by a rotor overcurrent. The crowbar can be disabled manually by the user when safe circumstances are reestablished.

C. RSC Control

The RSC provides decoupled control of stator active and reactive power. A cascade vector control structure with inner current control loops is applied. The overall control structure is shown in Fig. 2. When adopting stator-voltage-oriented (SVO) control, a decomposition in d and q components is performed ($V_{sq} = 0$). Neglecting the stator resistive voltage drop, the stator output active and reactive powers are expressed as

$$P_s \approx \frac{3}{2}\frac{L_h}{L_s} V_{sd} I_{rd} \tag{20}$$

$$Q_s \approx -\frac{3}{2}\frac{V_{sd}}{L_s}\left(\frac{V_{sd}}{\omega_s} + L_h I_{rq}\right) \tag{21}$$

thus, the stator active and reactive power can be controlled independently, controlling the d and q components of the rotor current. Based on (20) and (21), the outer power control loops are designed.

D. LSC Control

The LSC controls the dc voltage $V_{\rm dc}$ and provides reactive power support. A voltage-oriented cascade vector control structure with inner current control loops is applied [see Fig. 2 (right)]. The line current I_l can be controlled by adjusting the voltage drop across the line inductance L_l giving the following dynamics:

$$V_s = R_l I_l + L_l \frac{dI_l}{dt} \tag{22}$$

which is used to design the current controller, while the dc voltage dynamics can be expressed by

$$C_{\rm dc}\frac{dV_{\rm dc}}{dt} = I_{\rm dc} - I_{\rm load} \tag{23}$$

which is used to design the outer dc voltage control loop, where $C_{\rm dc}$ is the dc capacitance and $I_{\rm dc}$ and $I_{\rm load}$ are the dc currents on LSC and RSC side, respectively.

III. DVR

A. Electrical System

A DVR is a voltage source converter equipped with a line filter (usually *LC* type). Usually, a coupling transformer is used in series to the grid in order to correct deteriorated line voltages to reduce possible problems on a sensitive load or generator. Different transformer-based topologies are compared with respect to the number of hardware components, switching harmonics, dc-link control, and the ability to inject zero sequence voltages in [31]. Different system topologies are investigated in regard to the connection of the dc link and the rating in power and voltage

in [22]. The rating of the DVR system depends mainly on the depth of the voltage fault that should be compensated. For voltage sags or swells with zero-phase angle jump, the requirement of active power of the DVR is simply given by

$$P_{\mathrm{DVR}} = \left(\frac{V_1 - V_2}{V_1}\right) P_{\mathrm{load}} \tag{24}$$

where V_1 is the nominal and V_2 the faulty line voltage. Note that special focus must be taken on voltage faults with phase angle jump that can lead to a higher power rating [21]. When the DVR compensates a voltage sag, the active power of the DFIG is partly fed into the grid and the DVR system that is dependent of the remaining grid voltage. The active power flowing into the DVR charges its dc link. The excess energy must either be delivered to an energy storage system or transformed into heat by a dc chopper. Note that for full compensation of a full voltage dip, the DVR must be rated for the power of the wind turbine, making the solution ineconomical. Thus, the solution will probably be implemented to fully compensate the line voltage during partial voltage dip or swell and to assist during full voltage dip.

The injection transformers have a great impact on the DVR design. To adapt the DVR dc voltage to the compensating voltage, an adequate transformer ratio must be chosen. The design of the injection transformers differs from normally used shunt transformers. They must be higher rated to avoid possible saturation effects and lower the risk of high inrush currents that must be handled by the converter. Rating and design issues for the injection transformer are given in [32].

In practical applications, several security issues must be considered. Since the DVR is connected in series to the load, bypass switches across the transformers must be included to disconnect the DVR from the load, to protect the converter from damage in overload situations.

The experimental 30 kVA DVR system used here is based on three single-phase full bridge voltage source converters using a common dc link. The topology allows the injection of zero-sequence voltages by using three single-phase injection transformers (see Table I). Special focus must be taken on the control and measurement setup. Small dc components in the output voltages can drive the injection transformers into saturation, resulting in high magnetization currents.

The phase voltages can be controlled independently, which is advantageous for further investigations in three-phase four-wire systems.

TABLE I
SIMULATION AND EXPERIMENTAL PARAMETERS

Simulation Parameters		
Symbol	Quantity	Value
U_{line}	low voltage level (phase-to-phase, rms)	690 V
ω_s	Line angular frequency	2 π 50 Hz
P_{DFIG}	Wind turbine rated power	2 MW
i	stator to rotor transmission ratio	1
n	Rated mechanical speed	1800 r/min
L_h	mutual inductance	3.7 mH
R_s	stator resistance	10 mΩ
$R_{crowbar}$	crowbar resistance	0.3 Ω
Experimental Parameters		
Symbol	Quantity	Value
U_{line}	grid voltage (phase-to-phase. rms)	330 V
P_{DFIG}	DFIG rated power	22 kW
n_{mech}	Mechanical speed	1800 r/min
N_{sr}	stator to rotor transmission ratio	1.5
L_h	mutual inductance	37.13 mH
R_s	stator resistance	112 mΩ
$R_{crowbar}$	crowbar resistance	2.7 Ω
V_{DC}	DVR DC voltage	560 V
n	series transformer ratio (DVR to line)	$\sqrt{3}$
C_{DC}	DVR DC link capacitance	7.5 mF

B. DVR Control

For control of the DVR system, a closed-loop control in a rotating *dq* reference frame is introduced in [22], but identified as unsuitable for the compensation of unsymmetrical grid faults. Because the majority of faults on a power system are unbalanced in nature, which results in unbalanced voltages, appropriate generation of unsymmetrical compensation voltage components by the DVR is an important feature. Thus, in [24], stationary-frame controllers for DVR implementation are designed to achieve good positive- and negative-sequence voltage regulation. The cascade control structure includes inner proportional current controllers. As outer voltage controllers proportional + resonant (P+Res) controllers are compared to H_∞-controllers. Multiloop controllers using a similar control structure with outer P+Res voltage controllers and inner PID current controllers with filter capacitor voltage feedback are presented in [25]. Both control structures have good steady-state sinusoidal error tracking of the positive- and negative-sequence voltage components. Anyway, Ibrahim et al. [28] describe that DVR current control is inadequate if the load is current-controlled too. Therefore, P+Res voltage controllers that are controlling directly the voltage across the filter capacitors without inner current controllers are used here.

The controller transfer function expressed in terms of inverter voltage reference u_i^*, measured filter capacitor voltage u_c, and filter capacitor voltage reference u_c^* is given by

$$u_i^*(s) = u_c(s) + G_{\mathrm{P+Res}}(s) \cdot (u_c^*(s) - u_c(s)) \tag{25}$$

where a feedforward of the measured filter capacitor voltage is used. The transfer function of the P+Res voltage controller is defined as

$$G_{\mathrm{P+Res}}(s) = K_P + K_I \frac{s}{s^2 + \omega_0^2} \tag{26}$$

which has been implemented in the discrete form leading to the following transfer function:

$$G_{\mathrm{P+Res}}(z) = K_{\mathrm{P}} + K_{\mathrm{I}} \frac{zT_{\mathrm{S}} - T_{\mathrm{S}}}{z^2 + z\left(T_{\mathrm{S}}^2 \omega_0^2 - 2\right) + 1}. \tag{27}$$

Additionally, an antiwindup functionality has been added. The control parameters K_P and K_I were found by the analysis of bode plots and root loci of the given discrete controller. The inverter system has been discrete modeled consisting of a delay element in series with the transfer function of the *LC* line filter.

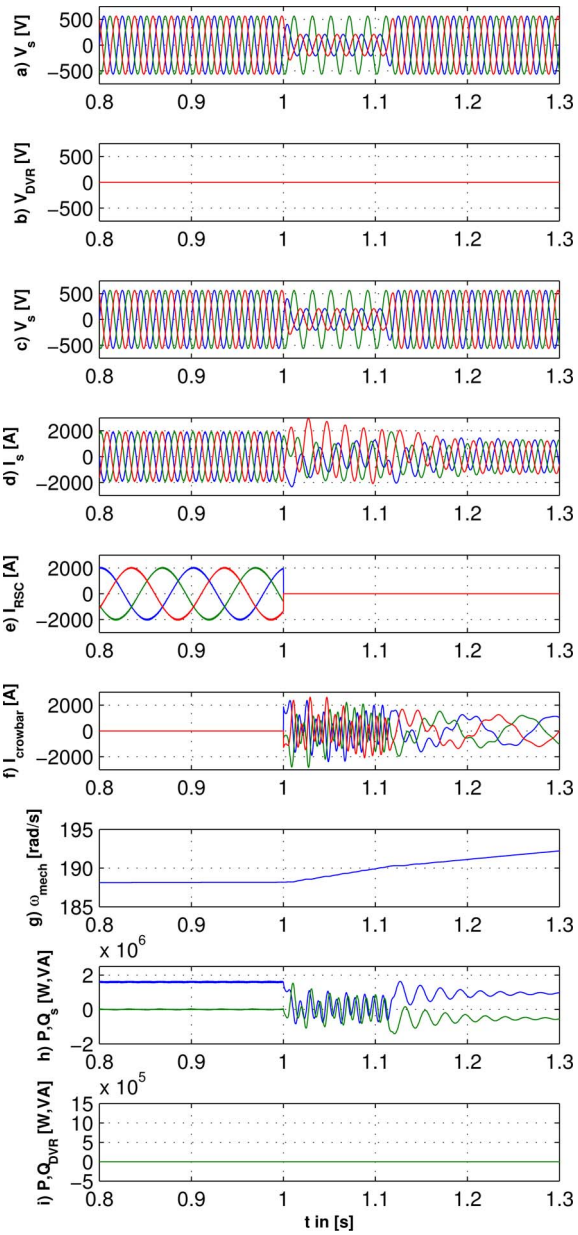

Fig. 3. Simulation of DFIG performance with crowbar protection during 37 % two-phase voltage dip. (a) Line voltage. (b) DVR voltage. (c) Stator voltage. (d) Stator current. (e) RSC current. (f) Crowbar current. (g) Mechanical speed. (h) Active and reactive stator power. (i) Active and reactive DVR power.

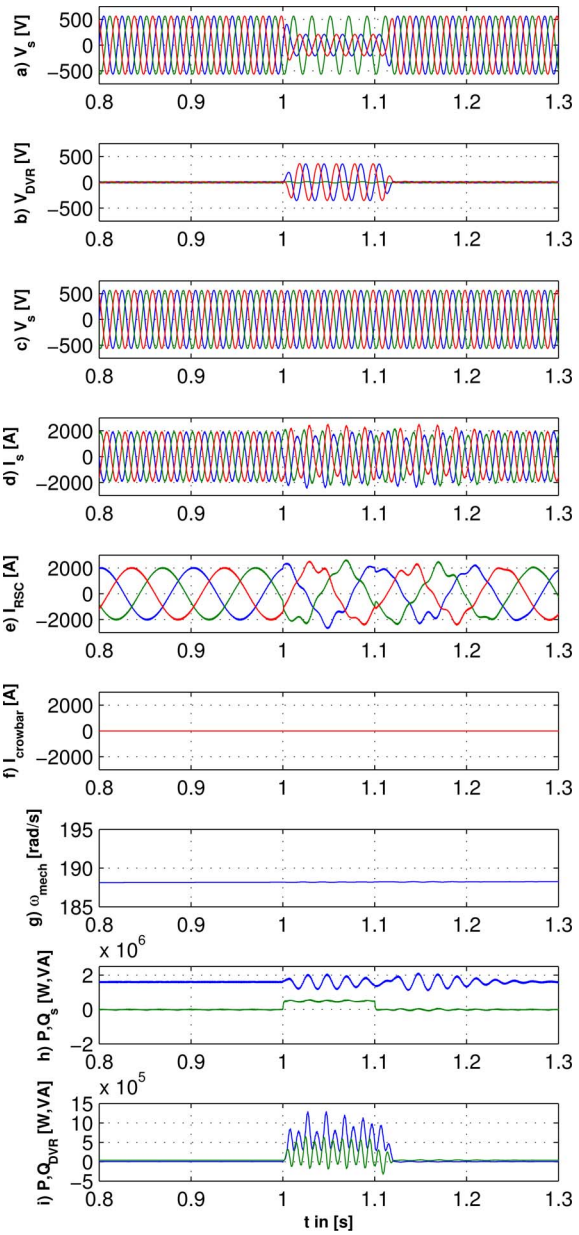

Fig. 4. Simulation of DFIG performance with DVR protection during 37 % two-phase voltage dip. (a) Line voltage. (b) DVR voltage. (c) Stator voltage. (d) Stator current. (e) RSC current. (f) Crowbar current. (g) Mechanical speed. (h) Active and reactive stator power. (i) Active and reactive DVR power.

IV. Simulation Results

To show the effectiveness of the proposed technique, simulations have been performed using MATLAB/Simulink and PLECS for a 2 -MW DFIG wind turbine system and a DVR, as shown in Fig. 1. The simulation parameters are given in Table I. The control structure, as shown in Fig. 2, is implemented in Simulink, while all power electronic components are modeled in PLECS.

The system performance of the DFIG is shown in Fig. 3, protected by the conventional passive crowbar, and in Fig. 4, protected by the DVR during a two-phase 37 % voltage dip of 100 ms duration [see Figs. 3(a) and 4 (a)]. The DFIG reacts with high stator currents I_s, and thus, high rotor currents are induced in the rotor circuit. When the rotor currents exceed the maximum level, the crowbar is triggered to protect the RSC from overcurrents I_{RSC} [see Fig. 3(e) and (f)].

When the voltage level has been reestablished and transients have decayed, the crowbar can be deactivated, which is not shown here. When the RSC is in operation, the machine magnetization is provided by the rotor, but when the crowbar is triggered, the RSC is disabled and the machine excitation is shifted to the stator. Thus, reactive power control cannot be provided during the voltage dip [see Fig. 3(h)], which is not acceptable when considering the grid codes. The machine cannot generate

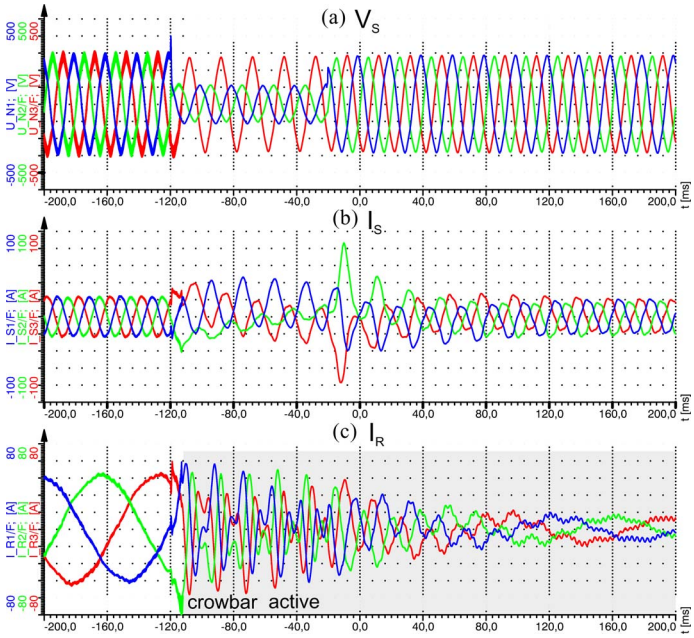

Fig. 5. Measurement results for DFIG with crowbar protection: (a) stator voltages, (b) stator currents, and (c) rotor currents.

enough torque so that the rotor accelerates, which can lead to disconnection of the turbine due to overspeed. The DVR is not activated in the simulations, as shown in Fig. 3.

When the wind turbine system is protected by the DVR, as shown in Fig. 4, the voltage dip can almost be compensated [see Fig. 4(c)]. The DFIG response is much less critical, which means that lower stator overcurrents and rotor overcurrents are produced so that the crowbar does not have to be triggered [see Fig. 4(d)–(f)]. Note that although the stator voltage dip is fairly well-compensated, a slight distortion in the stator currents (dc components), and thus, disturbed rotor currents can be observed. Anyway, the RSC remains in operation and can control stator active and reactive power independently. Thus, the speed is kept constant and a reactive power production ($Q_s = 0.5\,\mathrm{Mvar}$) during grid fault as demanded in grid codes is performed. Note that a communication between DVR and DFIG is necessary. In Fig. 4(i), the DVR power to compensate the voltage dip is shown. It becomes clear that the active and reactive power that cannot be fed into the faulty grid during grid fault must be consumed by the DVR.

V. Measurement Results

Measurement results are taken at a 22 kW test bench and a 30 kVA DVR connected in series to the grid. The schematic diagram of the laboratory setup is similar to the one shown in Fig. 1. The DVR converter is based on three single-phase full bridge voltage source converters using a common dc link (see Fig. 1). The dc link is charged with a passive six-pulse diode bridge and protected by a dc chopper. In the laboratory setup, the DVR is connected only to the stator of the machine; the LSC is connected to a separate faultless grid. The DFIG is driven by an industrial 18.5 kW induction machine drive to emulate the

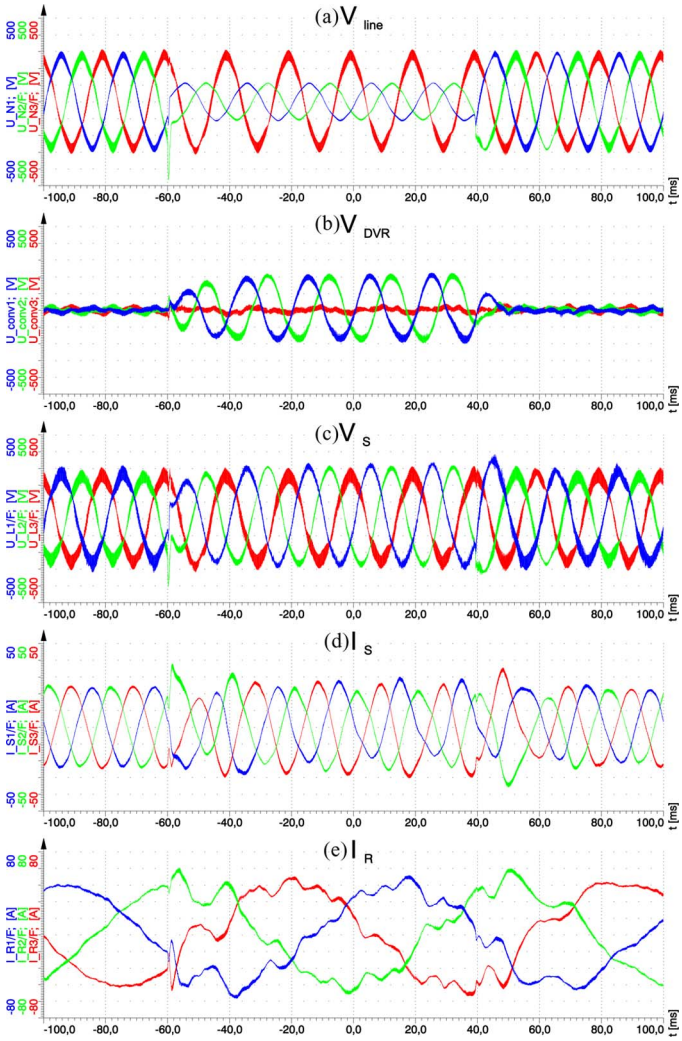

Fig. 6. Measurement results for DFIG with DVR protection: (a) line voltages, (b) DVR voltages, (c) stator voltages, (d) stator currents, and (e) rotor currents.

wind. The two-phase 37 % grid voltage dip (from 330 to 125 V) of 100 ms duration is generated by a transformer-based voltage sag generator, as described in [33].

In all laboratory tests, the grid voltage level has been lowered to 330 V (line to line) by a separate transformer to avoid saturation problems in the series-connected transformers of the DVR. The results have been recorded with a Dewetron data acquisition device. For both tests, the DFIG is operated supersynchronous with a slip of $s = -0.2$ (mechanical speed of 1800 r/min), feeding an active stator power of $P_s = 10\,\mathrm{kW}$ to the grid. If the LSC would be connected to the same point as the stator like in a real wind turbine system, the grid currents flowing through the DVR into the grid would be the sum of the LSC and stator currents. Thus, the DVR must be designed to handle these currents and the LSC control should be designed to create no transients, which is not focused here.

Without DVR, the RSC of the DFIG must be protected by the crowbar from overcurrents, as shown in Fig. 5(c), where the crowbar is triggered when the rotor currents exceed the critical limit of $I_r = 80$ A. The stator currents contain dc components

and the rotor currents have $\omega_{\mathrm{mech}} = 60\,\mathrm{Hz}$ components superimposed. The rotor currents decay with the stator time constant of $\tau_s \approx L_h/R_s = 330\,\mathrm{ms}$. When the voltage dip is cleared, after 100 ms, high stator currents are generated and the machine continues with inductive reactive power consumption that leads to a slight decrease of stator voltage amplitude.

The same two-phase voltage dip is investigated and shown in Fig. 6, but here, the DFIG is protected by the series-connected DVR. At nominal operation, the DVR does not compensate the line voltage. The DVR voltages are only slightly distorted by the grid voltage harmonics of the laboratory grid. When the voltage dip occurs, the DVR compensates the missing voltage in the two phases [see Fig. 6(b)] so that the stator voltage [see Fig. 6(c)] is only slightly affected by the voltage dip. No mentionary overcurrents are generated in the stator or rotor currents and the DFIG can continue directly its nominal operation feeding active power. Note that in the laboratory, the generator is always operated at unity power factor. For a reactive power production, according to the grid codes, a communication between DVR and DFIG would be necessary. The simulation and measurement results show a very similar behavior.

The results of this investigation show that the DVR can fully protect the DFIG system from asymmetrical grid voltage faults to allow uninterruptible low-voltage ride-through. One can conclude that the DVR can compensate voltage dips and swells of symmetrical and asymmetrical nature to allow a low- or high-voltage ride-through for any distributed load.

VI. Conclusion

The application of a DVR connected to a wind-turbine-driven DFIG to allow uninterruptible fault ride-through of grid voltage faults is investigated. The DVR can compensate the faulty line voltage, while the DFIG wind turbine can continue its nominal operation and fulfill any grid code requirement without the need for additional protection methods. The DVR can be used to protect already installed wind turbines that do not provide sufficient fault ride-through behavior or to protect any distributed load in a microgrid. Simulation results for a 2 MW wind turbine under an asymmetrical two-phase grid fault show the effectiveness of the proposed technique in comparison to the low-voltage ride-through of the DFIG using a crowbar where continuous reactive power production is problematic. Measurement results under transient grid voltage dips on a 22 kW laboratory setup are presented to verify the results.

References

[1] M. Tsili and S. Papathanassiou, "A review of grid code technical requirements for wind farms," *Renewable Power Generat., IET*, vol. 3, no. 3, pp. 308–332, Sep. 2009.

[2] R. Pena, J. Clare, and G. Asher, "Doubly fed induction generator using back-to-back pwm converters and its application to variable-speed wind-energy generation," *Electr. Power Appl., IEE Proc.*, vol. 143, no. 3, pp. 231–241, May 1996.

[3] S. Muller, M. Deicke, and R. De Doncker, "Doubly fed induction generator systems for wind turbines," *IEEE Ind. Appl. Mag.*, vol. 8, no. 3, pp. 26–33, May/Jun. 2002.

[4] J. Lopez, E. Gubia, P. Sanchis, X. Roboam, and L. Marroyo, "Wind turbines based on doubly fed induction generator under asymmetrical voltage dips," *IEEE Trans. Energy Convers.*, vol. 23, no. 1, pp. 321–330, Mar. 2008.

[5] M. Mohseni, S. Islam, and M. Masoum, "Impacts of symmetrical and asymmetrical voltage sags on dfig-based wind turbines considering phase-angle jump, voltage recovery, and sag parameters," *IEEE Trans. Power Electron.*, to be published.

[6] S. Seman, J. Niiranen, and A. Arkkio, "Ride-through analysis of doubly fed induction wind-power generator under unsymmetrical network disturbance," *IEEE Trans. Power Syst.*, vol. 21, no. 4, pp. 1782–1789, Nov. 2006.

[7] W. Zhang, P. Zhou, and Y. He, "Analysis of the by-pass resistance of an active crowbar for doubly-fed induction generator based wind turbines under grid faults," in *Proc. Int. Conf. Electr. Mach. Syst. (ICEMS)*, Oct., 2008, pp. 2316–2321.

[8] G. Pannell, D. Atkinson, and B. Zahawi, "Minimum-threshold crowbar for a fault-ride-through grid-code-compliant dfig wind turbine," *IEEE Trans. Energy Convers.*, vol. 25, no. 3, pp. 750–759, Sep. 2010.

[9] J. Morren and S. de Haan, "Short-circuit current of wind turbines with doubly fed induction generator," *IEEE Trans. Energy Convers.*, vol. 22, no. 1, pp. 174–180, Mar. 2007.

[10] J. Yang, J. Fletcher, and J. O'Reilly, "A series-dynamic-resistor-based converter protection scheme for doubly-fed induction generator during various fault conditions," *IEEE Trans. Energy Convers.*, vol. 25, no. 2, pp. 422–432, Jun. 2010.

[11] A. Causebrook, D. Atkinson, and A. Jack, "Fault ride-through of large wind farms using series dynamic braking resistors (march 2007)," *IEEE Trans. Power Syst.*, vol. 22, no. 3, pp. 966–975, Aug. 2007.

[12] P. Flannery and G. Venkataramanan, "Unbalanced voltage sag ride-through of a doubly fed induction generator wind turbine with series grid-side converter," *IEEE Trans. Ind. Appl.*, vol. 45, no. 5, pp. 1879–1887, Sep./Oct. 2009.

[13] J. Liang, W. Qiao, and R. Harley, "Direct transient control of wind turbine driven dfig for low voltage ride-through," in *Proc. IEEE Power Electron. Mach. Wind Appl. (PEMWA)*, Jun. 2009, pp. 1–7.

[14] D. Xiang, L. Ran, P. Tavner, and S. Yang, "Control of a doubly fed induction generator in a wind turbine during grid fault ride-through," *IEEE Trans. Energy Convers.*, vol. 21, no. 3, pp. 652–662, Sep. 2006.

[15] F. Lima, A. Luna, P. Rodriguez, E. Watanabe, and F. Blaabjerg, "Rotor voltage dynamics in the doubly fed induction generator during grid faults," *IEEE Trans. Power Electron.*, vol. 25, no. 1, pp. 118–130, Jan. 2010.

[16] P. Zhou, Y. He, and D. Sun, "Improved direct power control of a dfig-based wind turbine during network unbalance," *IEEE Trans. Power Electron.*, vol. 24, no. 11, pp. 2465–2474, Nov. 2009.

[17] G. Abad, M. Rodriguez, G. Iwanski, and J. Poza, "Direct power control of doubly-fed-induction-generator-based wind turbines under unbalanced grid voltage," *IEEE Trans. Power Electron.*, vol. 25, no. 2, pp. 442–452, Feb. 2010.

[18] L. Xu, "Coordinated control of dfig's rotor and grid side converters during network unbalance," *IEEE Trans. Power Electron.*, vol. 23, no. 3, pp. 1041–1049, May 2008.

[19] D. Santos-Martin, J. Rodriguez-Amenedo, and S. Arnaltes, "Providing ride-through capability to a doubly fed induction generator under unbalanced voltage dips," *IEEE Trans. Power Electron.*, vol. 24, no. 7, pp. 1747–1757, Jul. 2009.

[20] J. Lopez, E. Gubia, E. Olea, J. Ruiz, and L. Marroyo, "Ride through of wind turbines with doubly fed induction generator under symmetrical voltage dips," *IEEE Trans. Ind. Electron.*, vol. 56, no. 10, pp. 4246–4254, Oct. 2009.

[21] M. H. J. Bollen, *Understanding Power Quality Problems Voltage Sags and Interruptions*. New York: Wiley, 2000.

[22] J. Nielsen and F. Blaabjerg, "A detailed comparison of system topologies for dynamic voltage restorers," *IEEE Trans. Ind. Appl.*, vol. 41, no. 5, pp. 1272–1280, Sep./Oct. 2005.

[23] C. Meyer, R. De Doncker, Y. W. Li, and F. Blaabjerg, "Optimized control strategy for a medium-voltage dvr;theoretical investigations and experimental results," *IEEE Trans. Power Electron.*, vol. 23, no. 6, pp. 2746–2754, Nov. 2008.

[24] Y. W. Li, F. Blaabjerg, D. Vilathgamuwa, and P. C. Loh, "Design and comparison of high performance stationary-frame controllers for dvr implementation," *IEEE Trans. Power Electron.*, vol. 22, no. 2, pp. 602–612, Mar. 2007.

[25] F. Marafao, D. Colon, J. Jardini, W. Komatsu, L. Matakas, M. Galassi, S. Ahn, E. Bormio, J. Camargo, T. Monteiro, and M. Oliveira, "Multiloop controller and reference generator for a dynamic voltage restorer implementation," in *Proc. 13th Int. Conf. Harmon. Quality Power (ICHQP)*, Oct. 2008, pp. 1–6.

[26] D. Ramirez, S. Martinez, C. A. Platero, F. Blazquez, and R. M. de Castro, "Low-voltage ride-through capability for wind generators based on dynamic voltage restorers," *IEEE Trans. Energy Convers.*, to be published.
[27] C. Wessels and F. Fuchs, "High voltage ride through with facts for dfig based wind turbines," in *Proc. 13th Eur. Conf. Power Electron. Appl. (EPE)*, Sep. 2009, pp. 1–10.
[28] A. O. Ibrahim, T. H. Nguyen, D.-C. Lee, and S.-C. Kim, "Ride-through strategy for dfig wind turbine systems using dynamic voltage restorers," in *Proc. IEEE Energy Convers. Congr. Expo. (ECCE)*, Sep. 2009, pp. 1611–1618.
[29] C. Wessels, F. Gebhardt, and F. W. Fuchs, "Dynamic voltage restorer to allow lvrt for a dfig wind turbine," in *Proc. IEEE Int. Symp. Ind. Electron. (ISIE)*, Jul. 2010, pp. 803–808.
[30] M. P. Kazmierkowski, R. Krishnan, F. Blaabjerg, and D. Irwin, *Control in Power Electronics: Selected Problem* (Series in Engineering). New York: Academic, 2002.
[31] J. G. Nielsen, "Design and control of a dynamic voltage restorer," Ph.D. dissertation, Inst. Energy Technol., Aalborg Univ., Aalborg, Denmark, Mar. 2002.
[32] S. Mahesh, M. Mishra, B. Kumar, and V. Jayashankar, "Rating and design issues of dvr injection transformer," in *Proc. 23rd Annu. IEEE Appl. Power Electron. Conf. Expo. (APEC)*, Feb. 2008, pp. 449–455.
[33] C. Wessels, R. Lohde, and F. W. Fuchs, "Transformer based voltage sag generator to perform lvrt and hvrt tests in the laboratory," in *Proc. 14th Int. Power Electron. Motion Control Conf. (EPE/PEMC)*, Sep. 2010, pp. T11-8–T11-13.

Christian Wessels (S'08) was born in Hamburg, Germany, in 1981. He received the Dipl.-Ing. degree in 2007 from the Christian-Albrechts-University of Kiel, Kiel, Germany, where he is currently a Research Assistant in the Institute for Power Electronics and Electrical Drives.

His current research interests include wind turbine systems and FACTS converters.

Mr. Wessels was a corecipient of the Student Best Paper Award 2010 of the IEEE Industrial Electronics Society. He is a Student Member of the IEEE Power Electronics Society.

Fabian Gebhardt (S'10) was born in Kiel, Germany, in 1983. He received the Dipl.-Ing. degree in 2009 from the Christian-Albrechts-University of Kiel, Kiel, Germany, where he is currently a Research Assistant in the Institute for Power Electronics and Electrical Drives.

His current research interests include wind turbine systems and FACTS converters.

Mr. Gebhardt is a Student Member of the IEEE Power Electronics Society.

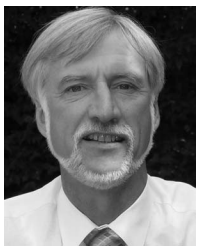

Friedrich Wilhelm Fuchs (M'96–SM'01) received the Dipl.-Ing. and Ph.D. degrees from the Rheinisch-Westfälische Technische Hochschule University of Technology, Aachen, Germany, in 1975 and 1982, respectively.

In 1975, he was with the University of Aachen, Aachen, Germany, where he was engaged in research on ac automotive drives. From 1982 to 1991, he was a Group Manager and engaged in research on development of power electronics and electrical drives in a medium-sized company. In 1991, he was a Managing Director in the Converter and Drives Division (presently Converteam), Allgemeine Elektrizitäts-Gesellschaft (AEG), Berlin, Germany, where he was engaged in research on design and development of drive products, drive systems, and high power supplies, covering the power range from 5 kVA to 50 MVA. In 1996, he joined as a Full Professor at the Christian-Albrechts-University of Kiel, Kiel, Germany, where he is currently the Head of the Institute for Power Electronics and Electrical Drives. He is the author or coauthor of more than 150 papers. His current research interests include power semiconductor application, converter topologies, variable-speed drives as well as their control; and renewable energy conversion, especially wind and solar energy, on nonlinear control of drives as well as on diagnosis of drives and fault-tolerant drives. Many research projects are carried out with industrial partners. His institute is a Member of CEwind eG, registered corporative, competence center of research in universities in wind energy Schleswig-Holstein, as well as of competence center for power electronics in Schleswig-Holstein (KLSH).

Prof. Fuchs is the Chairman of the Supervisory Board of Cewind, the Convenor [Deutsche Kommission Elektrotechnik Elektronik Informationstechnik (DKE), International Electrotechnical Commission (IEC)], International Speaker for Standardization of Power Electronics as well as a Member of Verband der Elektrotechnik Elektronik Informationstechnik (VDE) and European Power Electronics (EPE) and Drives Association.